Contents

VIP ***The following Communications have been judged by at least two referees to be "very important papers" and will be published online at www.angewandte.org soon:***

*T. Lewis, M. Faubel, B. Winter, J. C. Hemminger**
CO_2 Capture in an Aqueous Solution of an Amine: Role of the Solution Interface

*Y. H. Kim, S. Banta**
Complete Oxidation of Methanol in an Enzymatic Biofuel Cell by a Self-Assembling Hydrogel Created from Three Modified Dehydrogenases

R. B. Bedford, M. F. Haddow, C. J. Mitchell, R. L. Webster*
Mild C–H Halogenation of Anilides and the Isolation of an Unusual Pd^{I}–Pd^{II} Species

A. Bonet, C. Pubill-Ulldemolins, C. Bo, H. Gulyás,* E. Fernández**
Transition-Metal-Free Diboration by the Activation of Diboron Compounds with Simple Lewis Bases

*W. Liu, V. Khedkar, B. Baskar, M. Schürmann, K. Kumar**
Branching Cascades: A Concise Synthetic Strategy Targeting Diverse and Complex Molecular Frameworks

*M. Nakanishi, D. Katayev, C. Besnard, E. P. Kündig**
Synthesis of Fused Indolines by Palladium-Catalyzed Asymmetric C–C Coupling Involving an Unactivated Methylene Group

Editorial

Chemistry's Role in Regenerative Energy — R. Schlögl — **6424 – 6426**

Author Profile

"When I was eighteen I wanted to be a prosecutor. My first experiment was making sodium out of sodium chloride (electrolysis using my toy train set) …"
This and more about Stefan Bräse can be found on page 6444.

Stefan Bräse — **6444**

News


A. Bender


I. Ott


C. G. Hartinger


U. J. Meierhenrich


T. Ritter

Medicinal and Pharmaceutical Chemistry Prize: A. Bender and I. Ott — **6445**

Carl Duisberg Prize: C. G. Hartinger — **6445**

Horst Pracejus Prize: U. J. Meierhenrich — **6445**

BASF Catalysis Award: T. Ritter — **6446**

Highlights

Salt Effects

E. Hevia,* R. E. Mulvey* ____ 6448 – 6450

Split Personality of Lithium Chloride: Recent Salt Effects in Organometallic Recipes

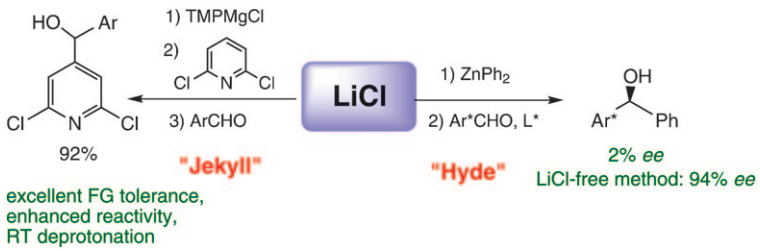

Jekyll and Hyde: Pinches of LiCl can catalyze orthometalations of halogen-substituted arenes and addition reactions of unsaturated esters, mediated by lithium diisopropylamide. Larger salt portions can transform weak organometallic bases (e.g., Grignard reagents, zincates) into "turbo" reagents of high reactivity and functional group tolerance. But the presence of LiCl, especially as an overlooked metathesis by-product can be detrimental to other catalytic reactions.

Essays

History of Chemistry

D. E. Lewis* ____ 6452 – 6458

A. M. Zaitsev: Lasting Contributions of a Synthetic Virtuoso a Century after his Death

A lasting legacy: A. M. Zaitsev (1841–1910) was a professor at Kazan University in Russia and discovered the sulfoxides and sulfonium salts. He synthesized the first lactone, expanded the synthesis of alcohols using alkylzinc nucleophiles, and carried out the first oxidation of an alkene with potassium permanganate. His students included three important organic chemists of the next generation: Wagner, Reformatskii, and Arbuzov.

Minireviews

Epigenetics

M. Münzel, D. Globisch, T. Carell* ____ 6460 – 6468

5-Hydroxymethylcytosine, the Sixth Base of the Genome

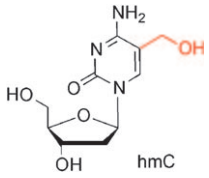

The sixth sense: 5-Hydroxymethylcytosine (hmC) was recently discovered as a new constituent of mammalian DNA, and besides 5-methylcytosine it is the only other modified base in higher organisms. This discovery shows that methylation of cyctosine is not a final step in gene silencing, but that further functionalization of the methyl group occurs.

For the USA and Canada:
ANGEWANDTE CHEMIE International Edition (ISSN 1433-7851) is published weekly by Wiley-VCH, PO Box 191161, 69451 Weinheim, Germany. Air freight and mailing in the USA by Publications Expediting Inc., 200 Meacham Ave., Elmont, NY 11003. Periodicals postage paid at Jamaica, NY 11431. US POSTMASTER: send address changes to *Angewandte Chemie*, Journal Customer Services, John Wiley & Sons Inc., 350 Main St., Malden, MA 02148-5020. Annual subscription price for institutions: US$ 9442/8583 (valid for print and electronic / print or electronic delivery); for individuals who are personal members of a national chemical society prices are available on request. Postage and handling charges included. All prices are subject to local VAT/sales tax.

Contents

Reviews

Ambident Reactivity

H. Mayr,* M. Breugst, A. R. Ofial ——— **6470 – 6505**

Farewell to the HSAB Treatment of Ambident Reactivity

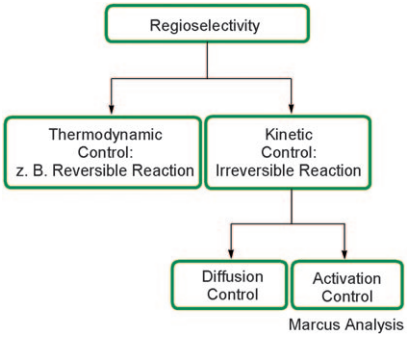

Hard or soft? The prediction of ambident reactivity by the concept of hard and soft acids and bases fails in the majority of cases and has to be abandoned. In this Review an alternative approach is presented to rationalize the regioselectivities of ambident systems which differentiates between kinetic and thermodynamic product control as well as between reactions proceeding with and without activation energy. The predictive power of qualitative Marcus theory is demonstrated.

Communications

Three-Dimensional Polymer Structures

X. Zhou, X. Wang, Y. Shen, Z. Xie, Z. J. Zheng* ——— **6506 – 6510**

Fabrication of Arbitrary Three-Dimensional Polymer Structures by Rational Control of the Spacing between Nanobrushes

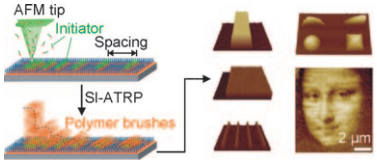

3D polymer structures can be fabricated by rational control of the spacing between nanosized polymer brushes. Each nanobrush can be precisely patterned by combination of dip-pen nanodisplacement lithography and surface-initiated atom transfer radical polymerization (SI-ATRP; see picture). Complex 3D topographic images of the Mona Lisa have been obtained in this way.

Protein Trans-Splicing

N. H. Shah, M. Vila-Perelló,* T. W. Muir* ——— **6511 – 6515**

Kinetic Control of One-Pot Trans-Splicing Reactions by Using a Wild-Type and Designed Split Intein

Charge-swapping of key intermolecular ion clusters in the naturally split DnaE intein from *Nostoc punctiforme* (Npu_{WT}) alters split intein binding affinities and trans-splicing kinetics. This concept was used to engineer the new split intein Npu_{MUT} with low cross-reactivity to Npu_{WT}. This intein pair can be used to catalyze multiple trans-splicing reactions in one pot with kinetically controlled selectivity (see picture).

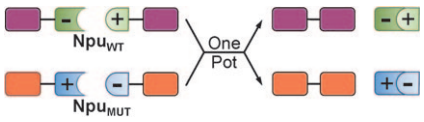

Protein–DNA Recognition

B. Bouvier, K. Zakrzewska, R. Lavery* ——— **6516 – 6518**

Protein–DNA Recognition Triggered by a DNA Conformational Switch

Making the switch: The analysis of molecular dynamics simulations of the SRY-protein–DNA complex shows that, when the SRY protein approaches the correct DNA target sequence, it triggers a DNA conformational switch and allows the passage from a nonspecifically bound to a specifically bound state (see picture; d_{AXC} = distance between DNA and SRY protein).

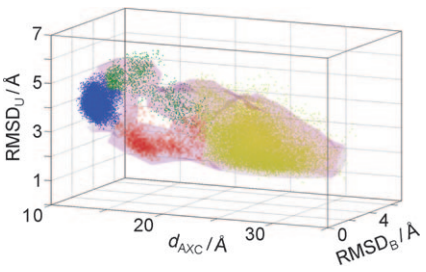

Wouldn't it be useful to have three arms? It came in handy for a trivalent sialic acid inhibitor, which blocked all three binding pockets of a trimeric adenoviral fiber-knob protein and thus prevented cell attachment and the subsequent infection of human corneal epithelial cells. The picture shows the terminal sialic acid moietes of the inhibitor bound to the top of the fiber head (C yellow, O red, N blue; the spacers and scaffold are not shown).

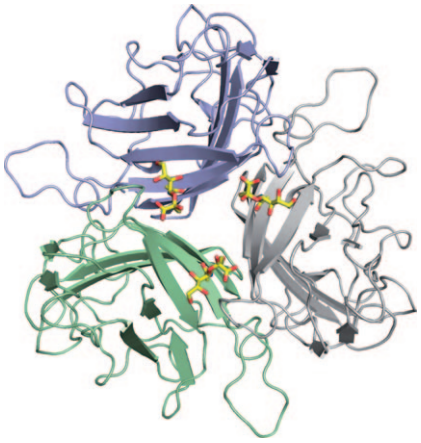

Drug Design

S. Spjut, W. Qian, J. Bauer, R. Storm, L. Frängsmyr, T. Stehle, N. Arnberg, M. Elofsson* ——— **6519 – 6521**

A Potent Trivalent Sialic Acid Inhibitor of Adenovirus Type 37 Infection of Human Corneal Cells

Double "click": Two different molecules can be sequentially immobilized on defined areas of the same surface by utilizing the different reactivity of activated and non-activated alkynyl groups (see picture). The reactions were carried out at room temperature in water, with the first immobilization step being catalyst-free and the second step requiring Cu^{I} as a catalyst.

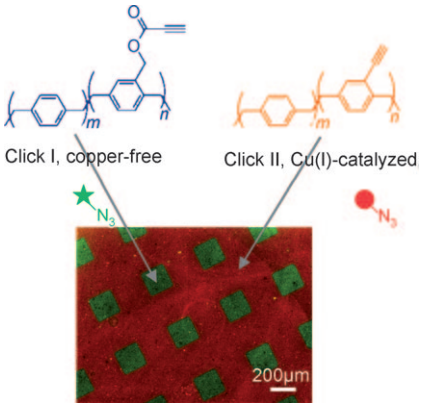

Bioactive Surfaces

X. Deng, C. Friedmann, J. Lahann* ——— **6522 – 6526**

Bio-orthogonal "Double-Click" Chemistry Based on Multifunctional Coatings

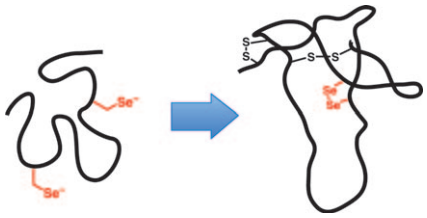

Secs for your folding problems: Selenocysteine (Sec) residues were used to drive the folding of conotoxin MrVIB, a previously "unfoldable" miniprotein with therapeutic potential (see picture). This simple strategy should generally facilitate the folding of peptides and proteins with multiple disulfide bonds.

Peptide Folding

A. D. de Araujo, B. Callaghan, S. T. Nevin, N. L. Daly, D. J. Craik, M. Moretta, G. Hopping, M. J. Christie, D. J. Adams, P. F. Alewood* ——— **6527 – 6529**

Total Synthesis of the Analgesic Conotoxin MrVIB through Selenocysteine-Assisted Folding

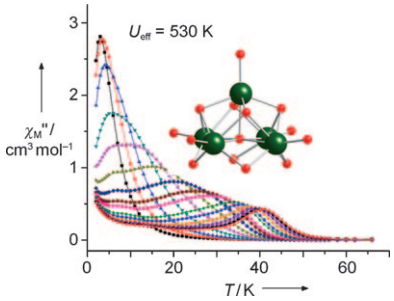

Single-molecule magnets: A square-pyramidal pentametallic dysprosium cluster (see picture) was synthesized and showed slow magnetic relaxation at temperatures as high as 40 K. The thermal energy barrier to relaxation of magnetization of this single-molecule magnet is 530 K and is the largest yet observed for any d- or f-block cluster compound.

Metal-Organic Frameworks

R. J. Blagg, C. A. Muryn, E. J. L. McInnes,* F. Tuna, R. E. P. Winpenny* **6530 – 6533**

Single Pyramid Magnets: Dy_5 Pyramids with Slow Magnetic Relaxation to 40 K

Contents

Protein Biosensors

N. Ayyadurai, N. Saravanan Prabhu, K. Deepankumar, S.-G. Lee, H.-H. Jeong, C.-S. Lee, H. Yun* ——— **6534 – 6537**

Development of a Selective, Sensitive, and Reversible Biosensor by the Genetic Incorporation of a Metal-Binding Site into Green Fluorescent Protein

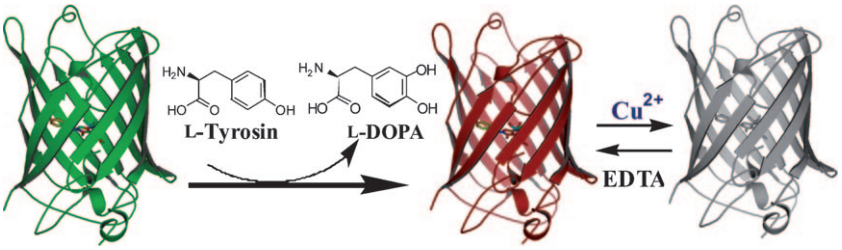

There when the light goes out: A copper biosensor was created by the introduction of the metal-chelating noncanonical amino acid L-DOPA in place of L-tyrosine into green fluorescent protein by genetic-code engineering (see picture). The specific binding of Cu^{2+} in vitro by the modified protein was reversible and resulted in fluorescence quenching in proportion to the amount of Cu^{2+} present. EDTA = ethylenediaminetetraacetic acid.

Nanocrystal Purification

J. D. Bass,* X. Ai, A. Bagabas, P. M. Rice, T. Topuria, J. C. Scott, F. H. Alharbi, H.-C. Kim, Q. Song,* R. D. Miller ——— **6538 – 6542**

An Efficient and Low-Cost Method for the Purification of Colloidal Nanoparticles

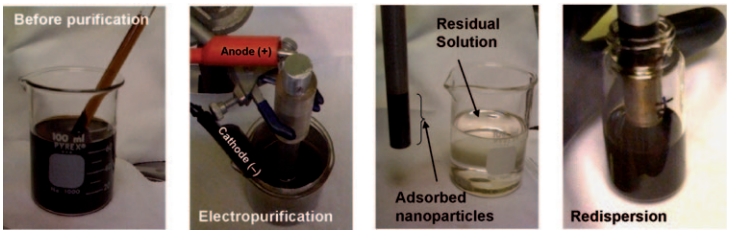

What a clean-up! A scalable method for the purification of nanoparticles in non-aqueous media has been developed that is based on reversible electrophoretic deposition (see picture). In this electropurification process, nanoparticles of varying size, shape, composition, and ligand environment can be electrodeposited onto an electrode surface, washed, and subsequently redispersed in as little as two minutes.

Metal–Organic Frameworks

C. Avendano, Z. Zhang, A. Ota, H. Zhao, K. R. Dunbar* ——— **6543 – 6547**

Dramatically Different Conductivity Properties of Metal–Organic Framework Polymorphs of Tl(TCNQ): An Unexpected Room-Temperature Crystal-to-Crystal Phase Transition

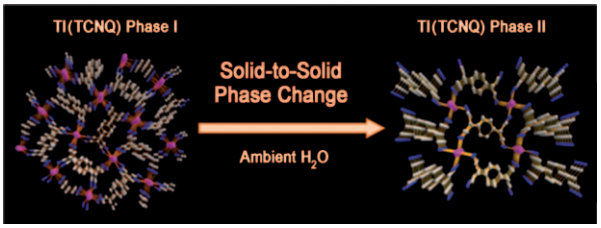

Just add water: Tl(TCNQ) polymorphs with very different charge-transport properties have been isolated, one of which undergoes a remarkable crystal-to-crystal phase transition to the second phase when exposed to ambient water vapor (see picture; TCNQ = tetracyanoquinodimethane).

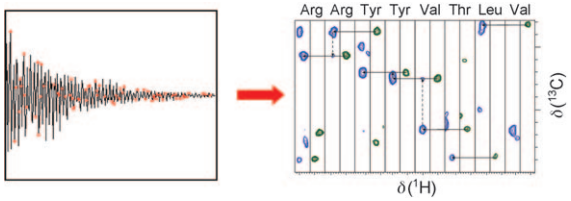

Make it snappy! The use of compressed sensing to reconstruct multidimensional NMR spectra enables significant reductions in recording time. Thus, 3D HNCA (blue) and HN(CO)CA spectra (green) of sufficient quality for rapid protein-backbone assignment were reconstructed from only 16% of the fully sampled data. The generality of the method and its robustness to noise should make it more broadly applicable, for example, to solid-state NMR spectroscopy.

NMR Spectroscopy

D. J. Holland, M. J. Bostock, L. F. Gladden, D. Nietlispach* ——— **6548 – 6551**

Fast Multidimensional NMR Spectroscopy Using Compressed Sensing

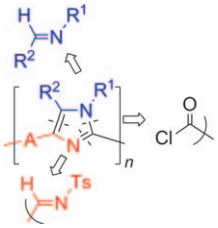

Just like tinkertoys: An alternative approach to access imidazole-containing π-conjugated materials is presented. The imidazole core was assembled at the same time as the oligomer by the palladium-catalyzed multicomponent coupling of imines, diimines, and di(acyl chloride)s, thus providing access to families of new conjugated materials, each formed in a one-step, catalytic reaction (see scheme; Ts = 4-toluenesulfonyl).

Oligomer Synthesis

A. R. Siamaki, M. Sakalauskas, B. A. Arndtsen* ——— **6552 – 6556**

A Palladium-Catalyzed Multicomponent Coupling Approach to π-Conjugated Oligomers: Assembling Imidazole-Based Materials from Imines and Acyl Chlorides

Extraordinary reaction rates and selectivity for the conversion of alkyl aromatic compounds, such as *p*-xylene, in terephthalic acid were observed for a heterogeneous perovskite catalyst of composition $(La,Sr)_{0.5}(Mn,Co)_{0.5}O_{2.38}$ (see picture). The oxygen-deficient catalyst was prepared by reduction of the oxygen-stoichiometric parent compound.

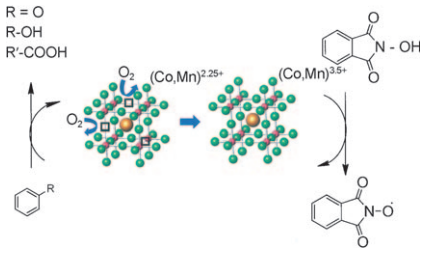

Perovskite Catalysts

A. Aguadero, H. Falcon, J. M. Campos-Martin, S. M. Al-Zahrani, J. L. G. Fierro, J. A. Alonso* ——— **6557 – 6561**

An Oxygen-Deficient Perovskite as Selective Catalyst in the Oxidation of Alkyl Benzenes

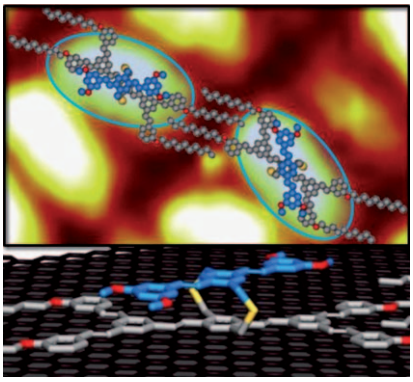

Janus faces: The Janus-like 3D tecton is a doubly functionalized molecular building block that consists of two different faces (see picture, gray: A and blue: B) linked by a rigid spacer. A is designed to act as a pedestal capable of guiding 2D self-assembly on the substrate, while B is a functional entity. This versatile approach allows for the creation of periodic arrays of functional units at a defined distance from the conductive substrate.

Self-Assembly

D. Bléger, F. Mathevet, D. Kreher, A.-J. Attias,* A. Bocheux, S. Latil, L. Douillard, C. Fiorini-Debuisschert, F. Charra* ——— **6562 – 6566**

Janus-Like 3D Tectons: Self-Assembled 2D Arrays of Functional Units at a Defined Distance from the Substrate

Contents

Tumor Imaging

K. Miki, A. Kimura, K. Oride, Y. Kuramochi, H. Matsuoka, H. Harada, M. Hiraoka, K. Ohe* ——— **6567 – 6570**

High-Contrast Fluorescence Imaging of Tumors In Vivo Using Nanoparticles of Amphiphilic Brush-Like Copolymers Produced by ROMP

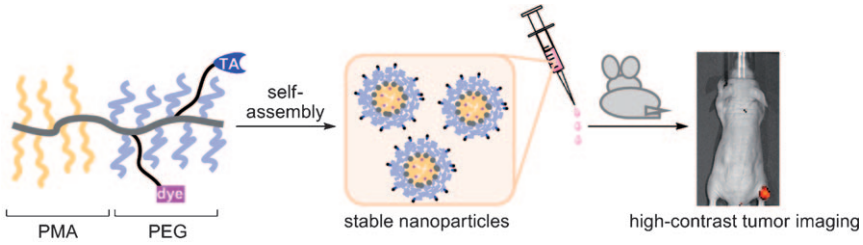

Nanoparticles at work: High-contrast tumor imaging of mice was performed by using copolymers with hydrophobic and hydrophilic polymer brushes that form cross-linked assemblies and show a highly stable core surface in aqueous media (see picture). Cyclic RGD peptides and glucosamine moieties were localized on the surface of the assemblies and acted as targeting agents (TA) that enhanced the accumulation of the assemblies in tumor tissues.

Organogold Compounds

S. Martínez-Salvador, J. Forniés,* A. Martín, B. Menjón ——— **6571 – 6574**

$[Au(CF_3)(CO)]$: A Gold Carbonyl Compound Stabilized by a Trifluoromethyl Group

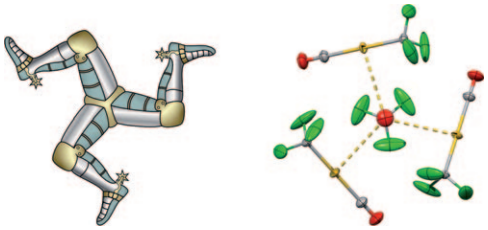

Fluorination operates for good: A trifluoromethyl group is able to stabilize the title compound (see picture; Au yellow, C gray, F green, O red), which formed by low-temperature treatment of $[PPh_4][Au(CF_3)_2]$ with $BF_3{\cdot}OEt_2$. A trigonal environment is adopted by each molecule with aurophilic interactions with three near-neighbors in a global triskelion arrangement.

Graphene

D. Yu, E. Nagelli, R. Naik, L. Dai* ——— **6575 – 6578**

Asymmetrically Functionalized Graphene for Photodependent Diode Rectifying Behavior

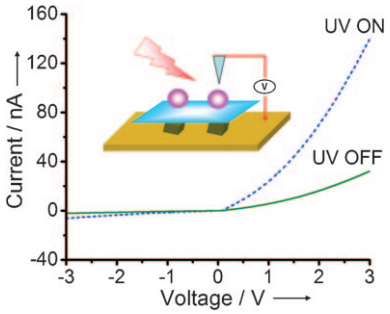

Both sides of the sheet: A simple method is described for functionalizing the two surfaces of individual graphene sheets with different nanoparticles in either a patterned or nonpatterned fashion. Graphene sheets with ZnO and Au nanoparticles on their opposite surfaces show a strong photodependent diodelike rectifying behavior (see picture; pink spheres = ZnO, green cubes = Au, blue triangle = AFM tip).

Negative Thermal Expansion

I. Yamada,* K. Tsuchida, K. Ohgushi, N. Hayashi, J. Kim, N. Tsuji, R. Takahashi, M. Matsushita, N. Nishiyama, T. Inoue, T. Irifune, K. Kato, M. Takata, M. Takano ——— **6579 – 6582**

Giant Negative Thermal Expansion in the Iron Perovskite $SrCu_3Fe_4O_{12}$

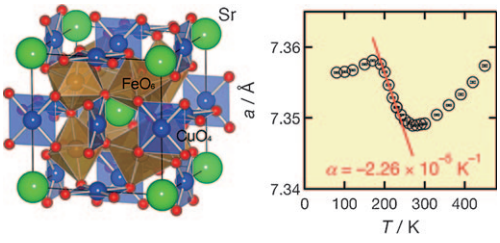

Big and cold: Strong internal compression of the Sr ion in the novel perovskite $SrCu_3Fe_4O_{12}$ (see structure) leads to giant negative thermal expansion (NTE) between 170 and 270 K. Mössbauer spectroscopy shows charge disproportionation of Fe^{IV} to Fe^{III} and Fe^{V} below 200 K. Thus, the isoelectric substitution of the *A*-site cation can induce a drastic change of the structural and electronic properties in $ACu_3Fe_4O_{12}$ perovskites.

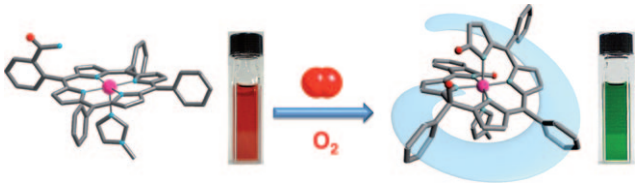

The turn of the screw: The Co^{II} complex of a porphyrin ligand with a pendant *ortho*-amidophenyl group converted into a helical Co^{III} complex with an acyclic pentapyrrole ligand upon addition of a coordinating base and exposure to O_2 (see picture, Co pink, N blue, O red, C gray). The enantiomers of the complex were separated and characterized, and preferential induction of an (*M*)-helical complex by addition of chiral bases was demonstrated.

Helical Structures

K. Yamanishi, M. Miyazawa, T. Yairi, S. Sakai, N. Nishina, Y. Kobori, M. Kondo,* F. Uchida ____ **6583 – 6586**

Conversion of Cobalt(II) Porphyrin into a Helical Cobalt(III) Complex of Acyclic Pentapyrrole

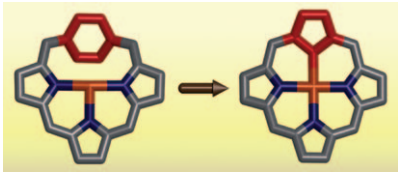

Feeling the contractions: Addition of palladium(II) and a hydroxide ion to a C–C double bond, β elimination, and competing cheletropic extrusion of carbon oxide and 1,2-hydride shift reactions lead to the contraction of *p*-phenylene to form a cyclopentadiene unit. This reaction results in the formation of a 21-carbaporphyrin from a palladium(II) *p*-benziporphyrin (see picture; C red/gray, N blue, Pd orange).

Porphyrinoids

B. Szyszko, L. Latos-Grażyński,* L. Szterenberg ____ **6587 – 6591**

A Facile Palladium-Mediated Contraction of Benzene to Cyclopentadiene: Transformations of Palladium(II) *p*-Benziporphyrin

Applaudable promiscuity: Racemase-type activity discovered for *B. cepacia* lipase with N-substituted α-aminonitriles is proposed to involve a C–C bond-breaking/forming mechanism in the hydrolase site of the enzyme, as supported by experimental data and calculations. This promiscuous activity in combination with the transacylation activity of the enzyme enabled the asymmetric synthesis of *N*-methyl α-aminonitrile amides in high yield (see scheme).

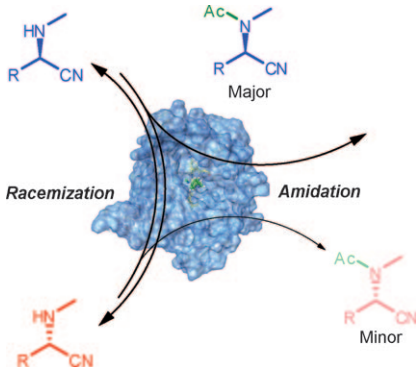

Dynamic Chemistry

P. Vongvilai, M. Linder, M. Sakulsombat, M. Svedendahl Humble, P. Berglund, T. Brinck, O. Ramström* ___ **6592 – 6595**

Racemase Activity of *B. cepacia* Lipase Leads to Dual-Function Asymmetric Dynamic Kinetic Resolution of α-Aminonitriles

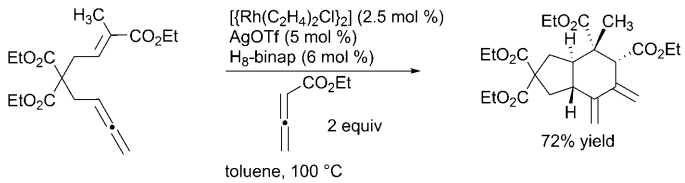

A complex situation: The title reaction was utilized for the construction of a variety of *trans*-fused hydrindanes and decalins in a highly convergent manner (see scheme; binap = 2,2′-bis(diphenylphosphanyl)-1,1′-binaphthyl, Tf = trifluoromethanesulfonate), with three σ bonds, two rings, and up to four contiguous stereocenters generated in a regio- and stereoselective fashion.

Synthetic Methods

A. T. Brusoe, E. J. Alexanian* ____ **6596 – 6600**

Rhodium(I)-Catalyzed Ene–Allene–Allene [2+2+2] Cycloadditions: Stereoselective Synthesis of Complex *trans*-Fused Carbocycles

Contents

Enantiomer Discrimination

T. Tu,* W. Fang, X. Bao, X. Li, K. H. Dötz ——— **6601 – 6605**

Visual Chiral Recognition through Enantioselective Metallogel Collapsing: Synthesis, Characterization, and Application of Platinum–Steroid Low-Molecular-Mass Gelators

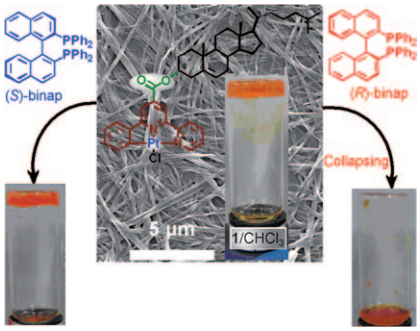

Seeing is believing: The visual chiral recognition of (*R*)- and (*S*)-binap has been realized through an enantioselective breakdown of metallogels prepared from novel aromatic–linker–steroidal-type pincer platinum gelators. Van der Waals interactions, π stacking, and metal–metal bonding are responsible for the aggregation and chiral recognition.

Magnetocaloric Effect

M. Evangelisti,* O. Roubeau, E. Palacios, A. Camón, T. N. Hooper, E. K. Brechin, J. J. Alonso ——— **6606 – 6609**

Cryogenic Magnetocaloric Effect in a Ferromagnetic Molecular Dimer

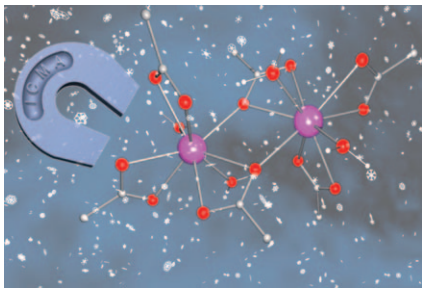

Molecoolers: An unprecedentedly large cryogenic magnetocaloric effect is observed in gadolinium acetate tetrahydrate (see picture, Gd pink, O red, C gray). The change in its magnetic entropy is ascribed to the high magnetic density combined with dominant ferromagnetism. For the first time in a molecular complex, direct measurements of the magnetocaloric effect corroborate indirect estimates based on heat capacity and magnetization.

Asymmetric Catalysis

J. Lv, L. Zhang, Y. Zhou, Z. Nie, S. Luo,* J.-P. Cheng ——— **6610 – 6614**

Asymmetric Binary Acid Catalysis: A Regioselectivity Switch between Enantioselective 1,2- and 1,4-Addition through Different Counteranions of In^{III}

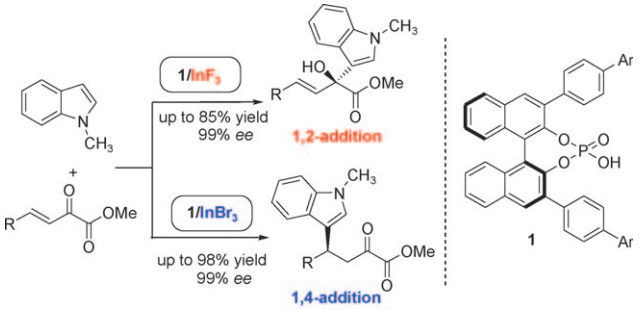

You can count on the anion: Simply swapping the anions of an indium Lewis acid leads to a remarkable regioselectivity switch between asymmetric 1,2- and 1,4-addition reactions. N-protected indoles and β,γ-unsaturated α-keto esters gave adducts with excellent enantioselectivity (see scheme).

Cyclic Polymers

X. Zhu, N. Zhou, Z. Zhang, B. Sun, Y. Yang, J. Zhu, X. Zhu* ——— **6615 – 6618**

Cyclic Polymers with Pendent Carbazole Units: Enhanced Fluorescence and Redox Behavior

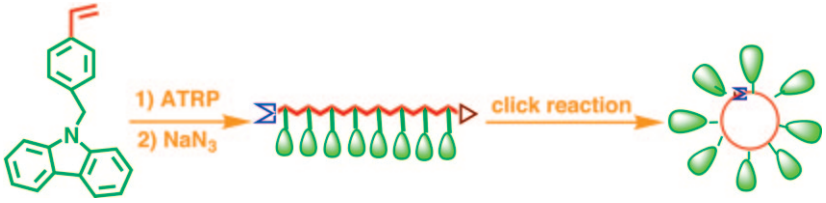

Circle the wagons: Well-defined cyclic poly(4-vinylbenzylcarbazole) (cyclic PVBCZ) polymers with differing molecular weights were prepared efficiently by successive atom-transfer radical polymerization (ATRP) and a click reaction (see picture; Σ = azide, Δ = alkynyl groups). The cyclic PVBCZ displayed a higher glass transition temperature than its linear precursor and has a higher fluorescence emission.

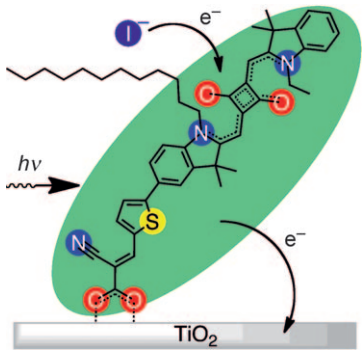

Squarely efficient: A squaraine sensitizer (see picture) shows an outstanding power conversion efficiency of 6.74% in liquid dye-sensitized solar cells and 2.69% in solid-state dye-sensitized solar cells. The high efficiencies are related to both the bathochromic shift of the absorption maximum compared to other squaraine sensitizers, and to the presence of additional absorptions that lead to high absorptivity over much of the visible spectrum.

Solar Cells

Y. Shi, R. B. M. Hill, J.-H. Yum, A. Dualeh, S. Barlow, M. Grätzel,* S. R. Marder,* Md. K. Nazeeruddin* ____ **6619 – 6621**

A High-Efficiency Panchromatic Squaraine Sensitizer for Dye-Sensitized Solar Cells

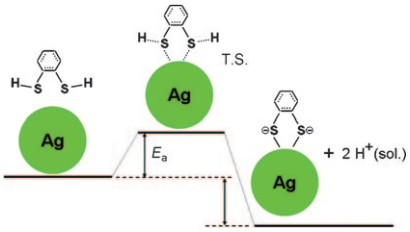

Reactions of thiols that are used to modify nanoparticle (NP) properties at the surface of noble-metal NPs involve an activation process. By detecting second harmonic generation from the Ag NP surface, the activation energy E_a for the adsorption of 1,2-benzenedithiol onto silver nanoparticles in colloids was determined to be 8.4 kcal mol^{-1} (see picture), which may arise from the transition state (T.S.) in the bonding reaction.

Silver Nanoparticles

W. Gan, B. L. Xu, H.-L. Dai* **6622 – 6625**

Activation of Thiols at a Silver Nanoparticle Surface

The oxidative Heck arylation of homoallylic alcohols affords adducts in good yields and regioselectivities owing largely to coordination between the catalyst and hydroxy group (see scheme). Moreover, the Heck intermediate can be intercepted by an intramolecular palladium-catalyzed olefin oxyannulation, thus leading to a wide range of α-aryltetrahydrofurans, including highly functionalized scaffolds.

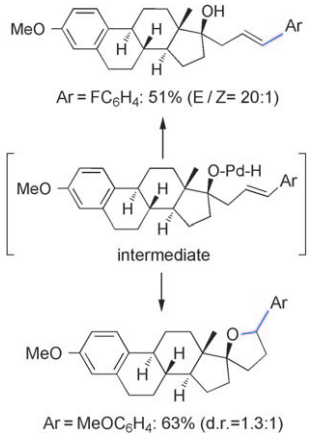

Olefin Functionalization

C. Zhu,* J. R. Falck ____ **6626 – 6629**

Alternative Pathways for Heck Intermediates: Palladium-Catalyzed Oxyarylation of Homoallylic Alcohols

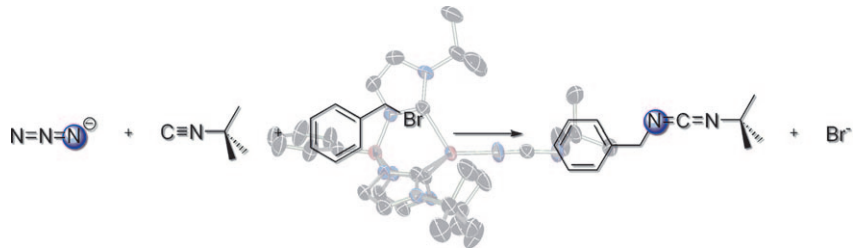

Degrees of separation: The extent of nitrogen atom transfer from iron(IV) nitrido complexes to unsaturated substrates is dictated by the supporting tris(carbene)borate ligand. This transfer step can be coupled to a subsequent group transfer reaction, creating a cycle for the synthesis of an unsymmetrical carbodiimide (see scheme).

Nitrogen Atom Transfer

J. J. Scepaniak, R. P. Bontchev, D. L. Johnson, J. M. Smith* **6630 – 6633**

Snapshots of Complete Nitrogen Atom Transfer from an Iron(IV) Nitrido Complex

Contents

Photophysics

G. J. Hedley, A. Ruseckas, A. Harriman, I. D. W. Samuel* ____ **6634 – 6637**

Conformational Effects on the Dynamics of Internal Conversion in Boron Dipyrromethene Dyes in Solution

Twisting the light away: Internal conversion between the S_2 and S_1 excited singlet states is rapid in the target dyes (see picture) but shows a clear sensitivity to rotational flexibility of the *meso*-phenyl ring. Steric crowding by methyl groups at the 4,7-positions leads to a curved S_2 potential-energy surface punctured with nonlocal pinholes coupled to the S_1 surface. Removal of these groups flattens the potential-energy surface, promoting barrierless crossing to the S_1 surface.

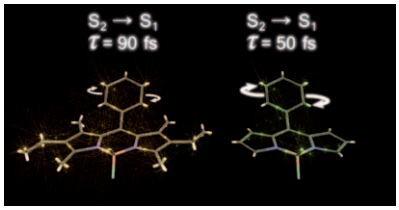

Aryne Chemistry

E. Yoshioka, S. Kohtani, H. Miyabe* ____ **6638 – 6642**

A Multicomponent Coupling Reaction Induced by Insertion of Arynes into the C=O Bond of Formamide

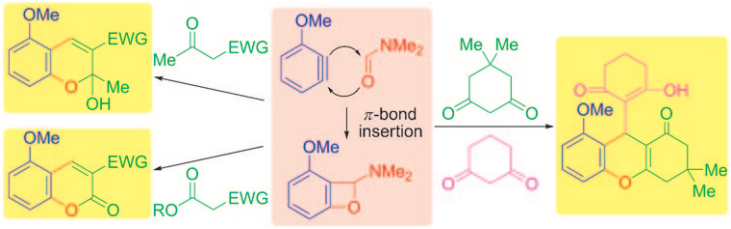

And aryne makes three: The three-component coupling of arynes, DMF, and active methylenes has provided an efficient method for the synthesis of 2*H*-chromene and coumarin derivatives (see scheme). The sequential multistep reactions are driven by the release of strain energy in the arynes and intermediates, and this finding was supported by thermodynamics.

Rotaxanes

S.-Y. Hsueh, J.-L. Ko, C.-C. Lai, Y.-H. Liu, S.-M. Peng, S.-H. Chiu* ____ **6643 – 6646**

A Metal-Free "Threading-Followed-by-Shrinking" Protocol for Rotaxane Synthesis

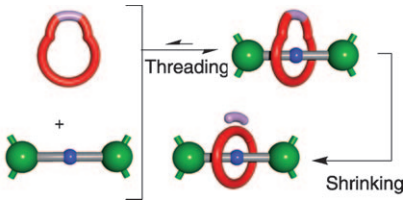

Shrinking ring size: Synthesis of a [2]rotaxane has employed photoextrusion of SO_2 from the arylmethyl sulfone motif of a [2]pseudorotaxane. A dumbbell-shaped guest molecule allows a shrinking reaction to decrease the number of atoms in the ring skeleton of the macrocyclic component of the [2]pseudorotaxane (see picture).

Macrobicyclic Phosphanes

M. Stollenz, M. Barbasiewicz, A. J. Nawara-Hultzsch, T. Fiedler, R. M. Laddusaw, N. Bhuvanesh, J. A. Gladysz* ____ **6647 – 6651**

Dibridgehead Diphosphines that Turn Themselves Inside Out

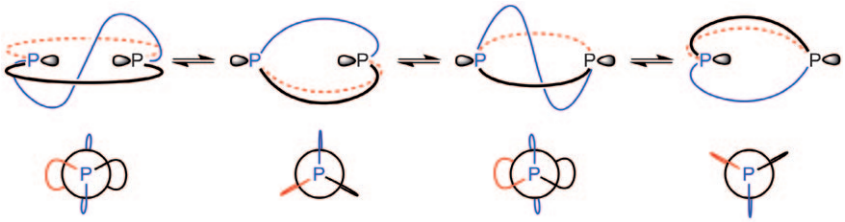

Molecular contortionists can lurk in unexpected places. The title compounds undergo equilibria that appear to involve straightforward pyramidal inversions at the phosphorus atoms, but in reality the stereoisomers interconvert by turning themselves inside out (see scheme)!

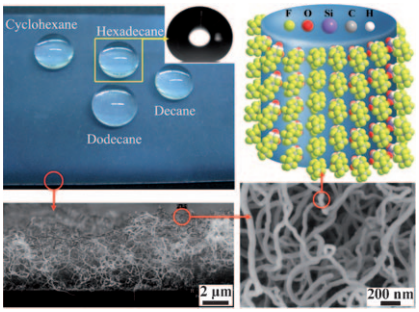

Superoleophobic surfaces were fabricated by using organosilanes. The surfaces feature high contact angles and ultralow sliding angles for various nonpolar liquids, excellent transparency, and chemical and environmental stability. The microstructure and superoleophobicity of the surfaces can be regulated simply by the water concentration in toluene used during the coating procedure.

Surface Chemistry

J. P. Zhang, S. Seeger ——— **6652 – 6656**

Superoleophobic Coatings with Ultralow Sliding Angles Based on Silicone Nanofilaments

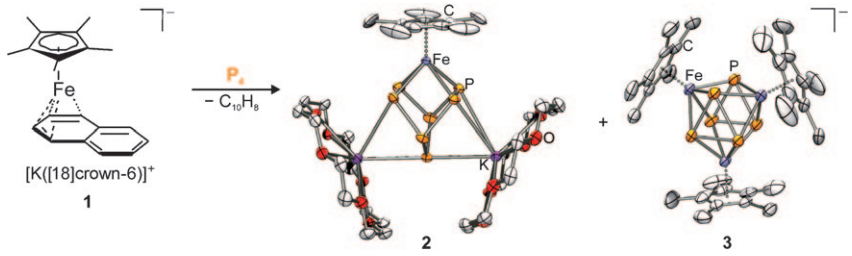

Transforming P_4: The reaction of the anionic Cp*Fe$^-$ equivalent **1** with white phosphorus is a promising new approach toward P_4 activation. The reaction proceeded under mild conditions and enabled the synthesis of remarkable anionic polyphosphido complexes. Two new iron polyphosphides **2** and **3** were isolated and characterized by X-ray crystallography, ^{31}P NMR spectroscopy, and quantum chemical calculations.

P_4 Activation

E.-M. Schnöckelborg, J. J. Weigand, R. Wolf* ——— **6657 – 6660**

Synthesis of Anionic Iron Polyphosphides by Reaction of White Phosphorus with "Cp*Fe$^-$"

Counterintuitive: The preformation of ion pairs can explain the low melting points of imidazolium-based ionic liquids (ILs) and the resulting expanded range of working temperatures. This quasi-ion-pair formation is possible for ILs having cations with only one interaction site leading to local and directional hydrogen bonds with the corresponding anion (see structure; O red, N blue, F green, S yellow).

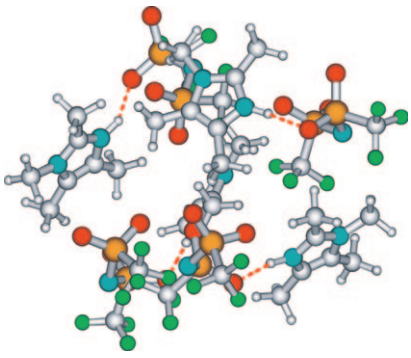

Ionic Liquids

T. Peppel, C. Roth, K. Fumino, D. Paschek, M. Köckerling,* R. Ludwig* ——— **6661 – 6665**

The Influence of Hydrogen-Bond Defects on the Properties of Ionic Liquids

Contents

Crystal Transformation

T. Tatic, S. Hermann, M. John, A. Loquet, A. Lange, D. Stalke* ——— **6666 – 6669**

Pure α-Metallated Benzyllithium from a Single-Crystal-to-Single-Crystal Transition

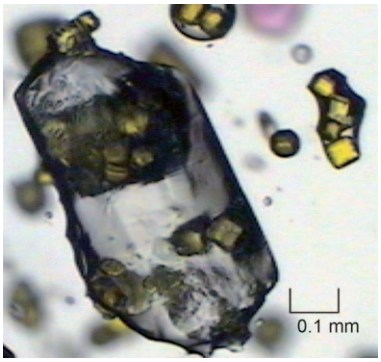

Crystal cannibalization: In a solution-mediated single-crystal-to-single-crystal transition the colorless starting material $[\{Me_2N(CH_2)_2OMe\}\cdot(LiCH_2SiMe_3)]_2$ converts in toluene into yellow crystals of the benzyllithium tetramer $[\{Me_2N(CH_2)_2OMe\}\cdot(LiCH_2C_6H_5)]_4$ (see picture, microscope photograph of the transforming crystals). A straightforward convenient access to commercially interesting benzyllithium in ligand-stabilized form is thus provided.

Supporting information is available on www.angewandte.org (see article for access details).

A video clip is available as Supporting Information on www.angewandte.org (see article for access details).

This article is available online free of charge (Open Access)

Service

Spotlight on Angewandte's Sister Journals ——— *6441 – 6443*

Vacancies ——— *6443*

Preview ——— *6671*